Effects of polarization on laser holography for microstructure fabrication

Hui Min Su, Y. C. Zhong, X. Wang, X. G. Zheng, J. F. Xu, and H. Z. Wang*
State Key Laboratory of Ultrafast Laser Spectroscopy, Zhongshan University, Guangzhou 510275, People's Republic of China
(Received 16 November 2001; revised manuscript received 2 January 2003; published 21 May 2003)

We perform a kind of computer stimulation on the multi-laser-beam interference. Using this method, we picture the interference patterns and describe the influence of the polarization of lights upon the clarity of the pattern. We find out the relations between the polarization states of the lights for the case of the best pattern and provide an optimal solution of the polarization on holographic lithography technology, and experiential formulas. This kind of analysis will improve the fabrication of submicrometer periodic structure efficiently.

DOI: 10.1103/PhysRevE.67.056619 PACS number(s): 42.40.−i, 42.40.Jv, 42.25.Ja, 42.70.Qs

I. INTRODUCTION

It is well known that periodic patterns with high resolution can be created by interference of multiple coherent laser beams, which is the so-called optical lattice. Following the fact that atoms and small dielectric particles can be trapped and cooled by laser beams, these patterns were applied as periodic optical traps with their centers at the intensity maximum spots [1–4]. Under proper conditions, the small dielectric particles will be subject to the force of local electromagnetic irradiance gradient and be trapped or arranged with the same periodicity as the optical lattice [5,6]. With a photoresist, the hologram recording can be obtained and the periodic electromagnetic field can produce periodic dielectric structures. In recent years, several kinds of microstructure have been fabricated successfully by holographic lithography with photoresist [7,8]. Since the intensity distribution in the volume of space defined by the overlapping beams can be described by classic Fourier transformation techniques, the hologram recording can be obtained by a small set of plane waves. Also, since the wave vectors of the laser beams determine the translational symmetry and lattice constant of the optical lattice, one can get a variety of intensity distributions in the interference pattern by modifying the wavelength and the incident angles of the beams [9–11]. While two- and three-beam interferences result in one-dimensional and two-dimensional periodic structures, respectively, four beams are required for three-dimensional periodic structures. It has been proved that almost all basic Bravais lattices can be formed by the antinodes produced in multibeam interference [11]. The other advantage of using interference is that the periods of the patterns may be as short as the optical wavelength. Since structures with lattice constants of micrometer or submicrometer dimensions play an essential role in photonics [12–14], the fabrication of structures with submicrometer periodicity has attracted much more attention in recent years. By comparison with other techniques, such as chemical vapor deposition [15], two-photon photopolymerization [16], semiconductor microfabrication [17–19], etc., the process of fabrication by holographic lithography is cheap, rapid, convenient, and effective. It is regarded as a promising method for microfabrication.

According to the theory of interference, the laser-beam wave vectors determine the translational symmetry and lattice constant of the interference. There remain several parameters, describing the polarization vectors of the beams, that are required to define the intensity distribution within a unit cell. The combination geometry of the polarization states has heavy infection on the contrast of the patterns. Several researchers have mentioned the generation of nets of vortices by multibeam interference [20,21] and the necessity of modulating the polarization of the coherence laser beam in the experiment and theory [7,11,22–24], but a detailed investigation has never been attempted.

In this paper, we study numerically the relationship between the polarization of lights and the clarity of the interference patterns. Instead of modulating the polarizations of the beams to create the optimal pattern through experiment, we performed some simulations on the multilaser-beam interference by a self-designed computer program and found out features of the transformation on the interference patterns efficiently. Here, we will show two cases as examples. They are the triangular interference pattern generated by three laser beams and the face-centered-cubic (FCC) interference pattern generated by four laser beams. Furthermore, we will present the optimal solution of the polarization in each case.

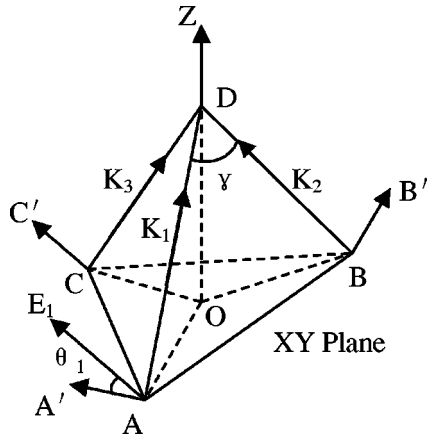

FIG. 1. Beam geometry for a 2D triangular interference pattern. Three laser beams are placed symmetrically around the Z axis and make an angle γ with each other. K_1, K_2, K_3 are the corresponding wave vectors. E_1 is the electric vector of the beam along the AO direction.

*Electronic address: stswhz@zsu.edu.cn

TABLE I. The optimal solutions for the case of $\gamma=\pi/12$.

θ_1 (rad)	θ_2 (rad)	θ_3 (rad)	V	I_{max}
0	$\pi/3$	$2\pi/3$	0.989	8.897
x	$x+\pi/3$	$x+2\pi/3$	0.989	8.897

II. THEORY

According to the principle of superposition, the interference between N laser beams presents the distribution figure of intensity $I(\vec{r})$ in the plane-wave expansion [23]:

$$I(\vec{r})=\left[\sum_{j=1}^{N}\vec{E}_j(\vec{r})\exp(i\vec{k}_j\cdot\vec{r})\right]\left[\sum_{j=1}^{N}\vec{E}_j^*(\vec{r})\exp(-i\vec{k}_j\cdot\vec{r})\right]$$
$$=\sum_{i=1}^{N}|\vec{E}_i|^2+\sum_{i\neq j}^{N}\vec{E}_i^*\cdot\vec{E}_j\exp[i(\vec{k}_j-\vec{k}_i)\cdot\vec{r}], \quad (1)$$

where $\vec{E}_j(\vec{r})$ and $\vec{k}_j$ are the complex amplitude and wave vector of the jth plane wave.

Equation (1) shows that the spatial periodicity of $I(\vec{r})$ is determined by the difference wave vectors $(\vec{k}_j-\vec{k}_i)$, while $2\leqslant N\leqslant 4$. The interference results in a $(N-1)$-dimensional pattern with its primitive reciprocal lattice vector $\vec{b}_m$ equal to $(\vec{k}_j-\vec{k}_i)$, where $m=1,2,\ldots,N-1$; $i,j=1,2,\ldots,N$; $i<j$. So we can vary the directions and the angles between the laser beams in order to get different spatial periodicity.

We should note that the second part in Eq. (1) defines the difference between the maximum and minimum intensities of the interference pattern, which, in turn, determines the contrast of the pattern. Therefore, our task is to investigate the relationship between the polarization states of each beam and the clarity of the interference pattern, and find out the optimal solution.

Given the wavelength and the electric field of each beam, our program stimulated the corresponding interference pattern according to the principle of plane-wave summation. Following the rules set up previously, the program evaluated the clarity of the interference patterns. After examining all the patterns by varying the polarization states of each beam, it picked out the clearest ones as the output.

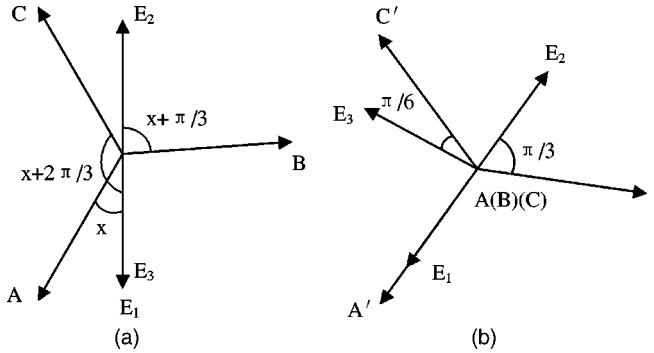

FIG. 2. The XY-plane projection of the electric vectors. The definitions of A,B,C,O are the same as those in Fig. 1. The following parameters were used: (a) $\gamma=\pi/12$, $\theta_1=x$, $\theta_2=x+\pi/3$, $\theta_3=x+2\pi/3$; (b) $\gamma=\pi/12$, $\theta_1=0$, $\theta_2=\pi/3$, $\theta_3=\pi/6$.

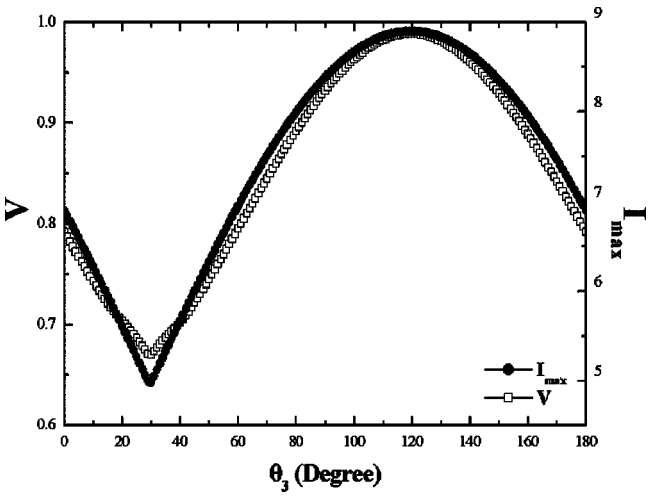

FIG. 3. The variation of V and I_{max} with θ_3 at $\gamma=\pi/12$, $\theta_1=0$, $\theta_2=\pi/3$.

We considered two aspects of the pattern for evaluation: the contrast, $V=(I_{max}-I_{min})/(I_{max}+I_{min})$, and the maximum intensity I_{max}. The former determines the quality of the pattern and the latter represents the efficiency on energy.

III. RESULTS AND DISCUSSIONS

In this section, we will show the results of stimulation on three- and four-beam interference. We considered two cases of three-beam interference, in which the angles between the incident waves were small or large.

A. Three-beam interference

Supposing the three laser beams follow

$$|\vec{k}_1|=|\vec{k}_2|=|\vec{k}_3|,\ |\vec{E}_1|=|\vec{E}_2|=|\vec{E}_3|=1. \quad (2)$$

Figure 1 shows the beam geometry of our stimulation on three-beam interference. The three laser beams are symmetrically placed around the Z axis, and make an angle γ with each other. The interference of those three beams results in a two-dimensional (2D) triangular pattern. AA' is a unit vector parallel to the OAD plane and perpendicular to $\vec{k}_1$. We de-

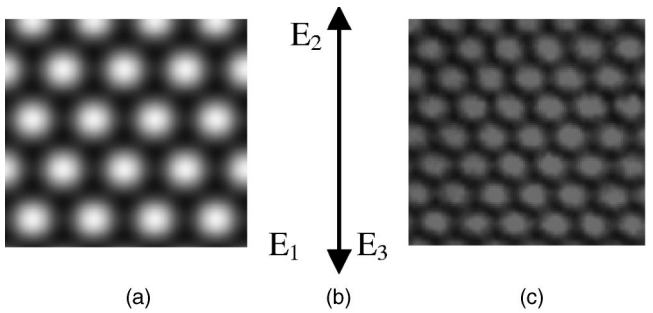

FIG. 4. Angular dependence of the interference pattern (the case of $\gamma=\pi/12$, $\theta_1=0$, $\theta_2=\pi/3$, $\theta_3=2\pi/3$).

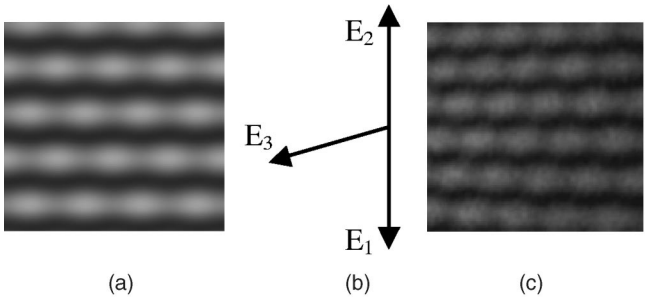

FIG. 5. Angular dependence of the interference pattern (the case of $\gamma=\pi/12$, $\theta_1=0$, $\theta_2=\pi/3$, $\theta_3=2\pi/9$).

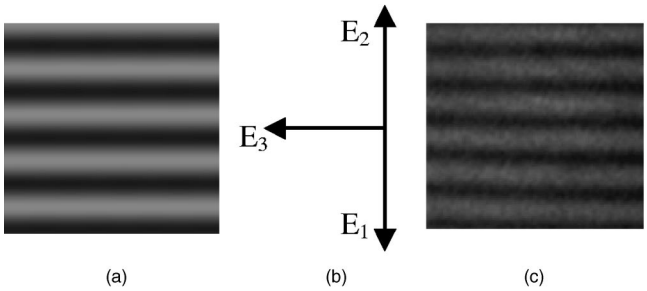

FIG. 6. Angular dependence of the interference pattern (the case of $\gamma=\pi/12$, $\theta_1=0$, $\theta_2=\pi/3$, $\theta_3=\pi/6$).

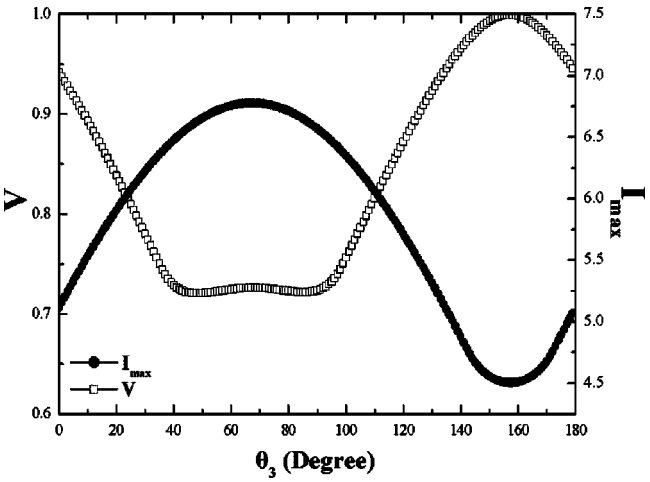

FIG. 7. The variation of V and I_{max} with θ_3 at $\gamma=\pi/3$, $\theta_1=17\pi/36$, $\theta_2=\pi/12$.

TABLE II. Part of the solutions for $V\approx 1$ in the case of $\gamma=\pi/3$.

θ_1 (rad)	θ_2 (rad)	θ_3 (rad)	V	I_{max}
$\pi/12$	$31\pi/36$	$17\pi/36$	0.999	4.51
$\pi/9$	$8\pi/9$	$\pi/2$	0.999	4.50
$5\pi/36$	$11\pi/12$	$19\pi/36$	0.999	4.51
$17\pi/36$	$\pi/12$	$31\pi/36$	0.999	4.51

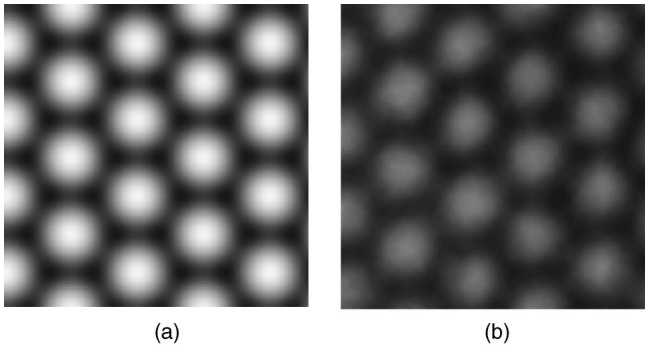

FIG. 8. The computer simulation images (a) and camera images (b) of the best interference patterns for the case of $\gamma=\pi/12$, $\theta_1=0$, $\theta_2=\pi/3$, $\theta_3=2\pi/3$.

fined θ_1 as the angle of $\vec{E}_1$ to the OAD plane originating from AA'. Also, we defined θ_2 and θ_3 as the angles of $\vec{E}_2$ to OBD and $\vec{E}_3$ to OCD, respectively.

Given the wavelength and the electric field of each beam, our program stimulated the corresponding interference pattern according to the principle of plane-wave summation. Following the rules set up previously, the program searches for the maximal and minimal values of the light intensity by Powell's quadratic convergent method [25] in the 2D (three-beam-interference) and 3D (four-beam-interference) space. After examining all the patterns by increasing the polarization states at a step of 5° from 0° to 180° for each beam, it picked out the clearest ones as the output.

Table I shows the optimal solutions on the condition that γ is small ($\gamma=\pi/12$). We should note that the best interference patterns appear in the case of

$$\theta_2-\theta_1=\theta_3-\theta_2=\pi/3. \tag{3}$$

It is demonstrated by Fig. 2(a) that such solutions make the XY-plane projections of the electric vectors remain in a line and then keep the electric vectors of each beam almost in one direction while γ is small enough. It results in the highest quality interference pattern.

Fixing θ_1 and θ_2 ($\theta_1=0,\theta_2=\pi/3$) as constants, we show contrast V and the maximum intensity I_{max} of the pattern as functions of θ_3 in Fig. 3. Both of them vary with periodicity of π and reach the extreme value at $\theta_3=2\pi/3$. Moreover, they decrease to the trough at $\theta_3=\pi/6$, which corresponds to $\vec{E}_3$ normal to $\vec{E}_1$ and $\vec{E}_2$ [Fig. 2(b)].

Figures 4–6, the computer simulation and the camera

TABLE III. Part of the optimal solutions for the case of $\gamma=\pi/3$.

θ_1 (rad)	θ_2 (rad)	θ_3 (rad)	V	I_{max}
0	$\pi/36$	$\pi/2$	0.93	6.03
0	$17\pi/36$	$35\pi/36$	0.93	6.03
$\pi/36$	$\pi/2$	0	0.93	6.03
$17\pi/36$	$35\pi/36$	0	0.93	6.03

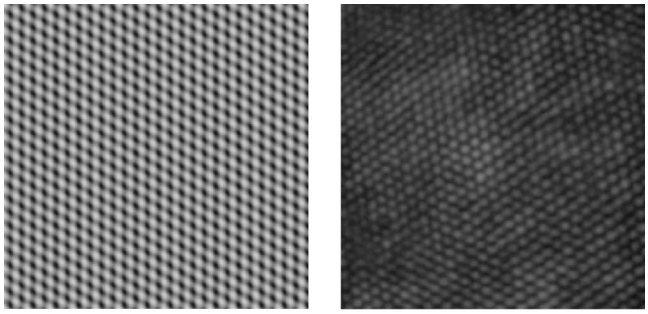

FIG. 9. The computer simulation images (a) and camera images (b) of the best interference patterns for the case of $\gamma=\pi/3$, $\theta_1=\pi/36$, $\theta_2=\pi/2$, $\theta_3=0$.

images of the intensity distribution, illustrate a serial evolution of the interference pattern from the best to the worst. As θ_3 changed from $2\pi/3$ to $\pi/6$, the intensity of each bright spot declined and their shapes stretched. Finally, the two-dimensional triangular pattern degenerated to a one-dimensional stripe pattern.

Next, the effect of polarization was examined at large γ ($\gamma=\pi/3$).

Fixing θ_1 and θ_2, we plot the variation of V and I_{max} with θ_3 in Fig. 7. At large γ, the peak of V and I_{max} separate for more than 80°. That means the solution we picked out could not satisfy the requirements of high pattern quality and high efficiency of energy at the same time. Furthermore, the maximum intensity decreases almost 50% at $V=1$ against that of $\gamma=\pi/12$, which represents the decline of energy efficiency. Moreover, the wave form of V is much more precipitous near the peak, which means a slight change in polarization states would lead to a sharp change in contrast.

Since lots of experiments concern a larger contrast value, we show several combinations of θ_1, θ_2, θ_3 corresponding to $V=1$ as optimal solutions in Table II.

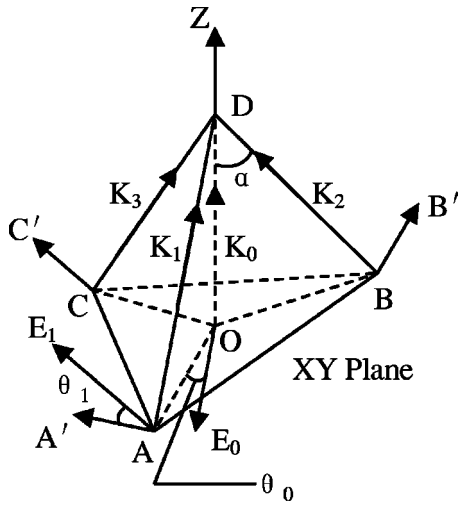

FIG. 10. Beam geometry for the fcc interference pattern. Three outer laser beams are placed symmetrically around the central beam and make an angle α of 38.9° with it. K_1, K_2, K_3, K_0 are the corresponding wave vectors.

TABLE IV. Part of the optimal solutions for the fcc interference pattern.

θ_0 (rad)	θ_1 (rad)	θ_2 (rad)	θ_3 (rad)	V	I_{max}
$\pi/9$	$\pi/9$	$4\pi/9$	$3\pi/4$	0.99	14.73
$\pi/9$	$\pi/9$	$4\pi/9$	$7\pi/4$	0.99	14.73
$5\pi/36$	$5\pi/36$	$17\pi/36$	$7\pi/9$	0.99	14.73
$5\pi/36$	$5\pi/36$	$17\pi/36$	$29\pi/36$	0.99	14.73

Also, considering both the contrast of the pattern and the energy efficiency, we present other combinations of θ_1, θ_2, θ_3 as optimal solutions in Table III. Picking out one of them to determine the polarization states of the three laser beams, we illustrate the interference pattern at $\gamma=\pi/3$ in Figs. 8(b) and 9(b), which is in sharp contrast to the case of $\gamma=\pi/12$ [Figs. 8(a) and 9(a)].

Furthermore, considering both the contrast of the pattern and the energy efficiency, we can get a series of optimal solutions for some γs (the range is from 0 to $\pi/2$). Based on the solutions, we can get experiential formulas by nonlinear fitting:

$$\theta_1=20,$$

$$\theta_2=0.004\,884\,101\,4\,\gamma^2-0.134\,527\,219\,\gamma+80.935\,477\,58,$$

$$\theta_3=0.006\,638\,005\,8\,\gamma^2-0.057\,774\,162\,\gamma+140.357\,612\,94. \tag{4}$$

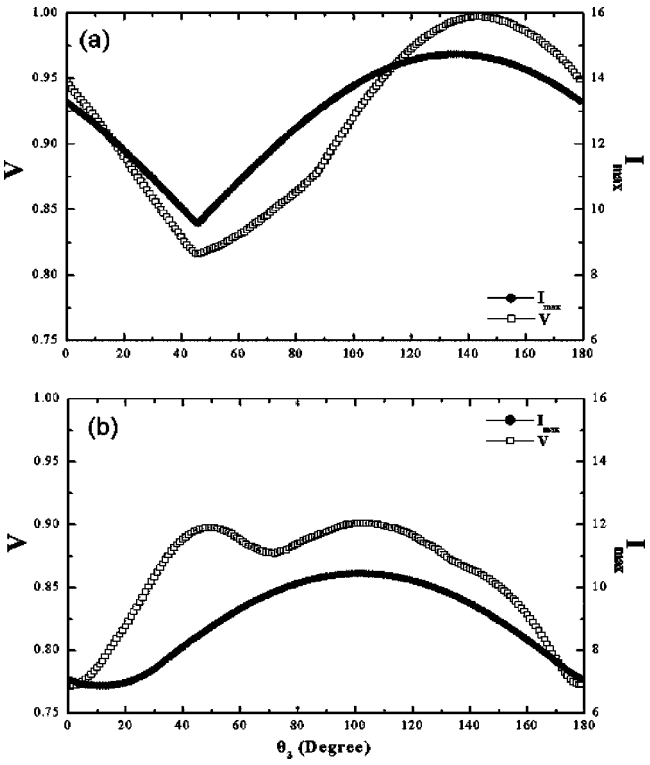

FIG. 11. The variation of V and I_{max} with θ_3 at an optimal solution (a) and a randomly selected one (b). The following parameters were used: (a) $\theta_0=\pi/9$, $\theta_1=\pi/9$, $\theta_2=4\pi/9$; (b) $\theta_0=5\pi/36$, $\theta_1=11\pi/12$, $\theta_2=35\pi/36$.

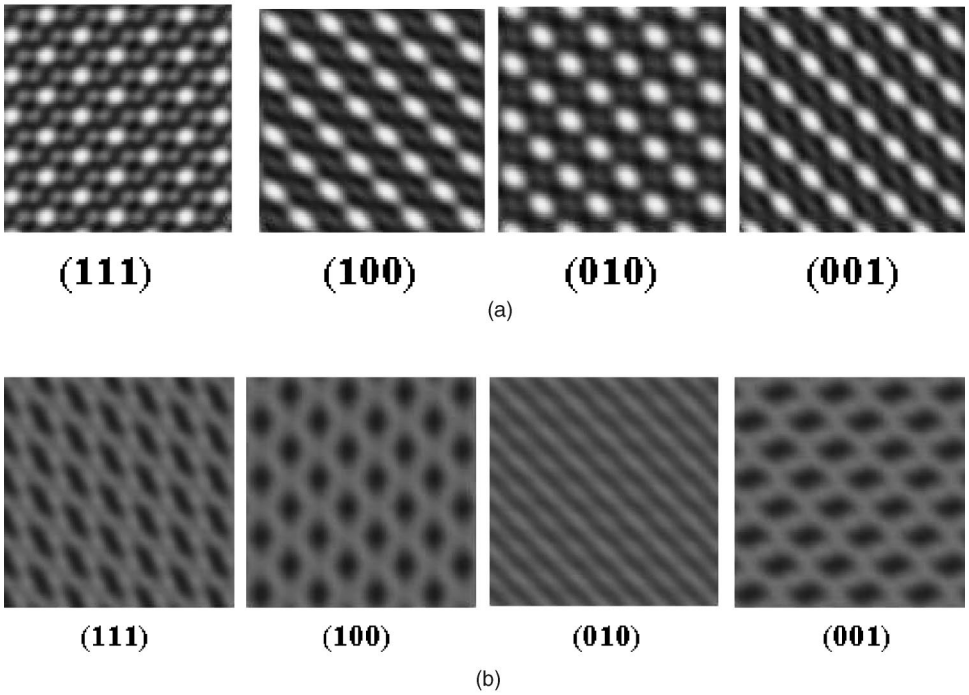

FIG. 12. The computer simulation images of the fcc interference pattern in the (100), (010), (001), and (111) planes at an optimal solution (a) and a randomly selected one (b). (a) $\theta_0=\pi/9$, $\theta_1=\pi/9$, $\theta_2=4\pi/9$, $\theta_3=7\pi/9$. (b) $\theta_0=5\pi/36$, $\theta_1=11\pi/12$, $\theta_2=35\pi/36$, $\theta_3=\pi/12$.

Using experiential formulas (4), it is very easy to get a good approximation of the optimal solutions (with large $\gamma=\pi/2$, which is the worst in the experiential formulas, it also can get combinations of $\theta_1=20$, $\theta_2=108$, $\theta_3=188$ to make $V=0.933\,486\,402\,034\,76$ and $I_{max}=4.765\,403\,747\,558\,59$).

B. Four-beam interference

Now, we investigate a fcc interference pattern produced by four laser beams. The beam geometry corresponding to such a pattern is shown schematically in Fig. 10. The three outer beams are symmetrically placed around the central beam and make an angle α of 38.9° with it. The electric field and the wave vector of each beam are defined as follows:

$$|\vec{k}_1|=|\vec{k}_2|=|\vec{k}_3|=|\vec{k}_0|,\ \ |\vec{E}_1|=|\vec{E}_2|=|\vec{E}_3|=|\vec{E}_0|=1. \quad (5)$$

The definitions of θ_1,θ_2, and θ_3 are the same as those in Fig. 1. Moreover, we define θ_0 as the angle between $\vec{E}_0$ and AA' originating from AA'.

Parts of the optimal solutions for fcc pattern are listed in Table IV. We obtained the parameters for a perfect interference, which satisfy the following relations:

$$|\theta_1-\theta_0|\leqslant\pi/18,\ \ |\theta_1-\theta_2-\pi/3|\leqslant\pi/18,$$

$$|\theta_3-\theta_2-\pi/3|\leqslant\pi/18. \quad (6)$$

As we mentioned before, these relations keep the electric vector of each beam in the directions misaligned by less than $\pi/18$. The variations of V and I_{max} with θ_3 are illustrated in Fig. 11. Figure 11(a) shows results using an optimal solution ($\theta_0=\pi/9,\theta_1=\pi/9,\theta_2=4\pi/9$) and a randomly selected solutions used for Fig. 11(b) ($\theta_0=5\pi/36$, $\theta_1=11\pi/12$, $\theta_2=35\pi/36$). The curves in Fig. 11(b) are much different from those in Fig. 11(a), including the position and the numerical value of the peaks and the wave form of curves.

To show the sharp difference between the fcc interference pattern created at the optimal solution and that created at a randomly selected one, Fig. 12 illustrates the computer stimulation image in the (100), (010), (001), and (111) planes. These pictures also validated the correctness of our stimulation program.

Using our theory result, we have already fabricated some fcc micrometer structure by a holographic lithography method combined with photoinduced polymerization. But we cannot provide the experimental results according to each plane listed above because of some technical difficulty in photography.

We have studied the close relationship between the polarization state of each beam and the quality of interference pattern. The results suggest that the alteration of the former leads to a wide range of the latter. The polarization states of the beams should be designed *a priori*, because of their considerable freedom in determining the distribution of intensity in a unit. We have induced experiential formulas for the three-beam interference. Although our discussion focused only on the two-dimensional triangular pattern and the fcc pattern, our procedure of stimulation applies to all the processes of multi-laser-beam interferences as well.

ACKNOWLEDGMENTS

This study was supported by the National Natural Science Foundation of China (Grant Nos. 19934002 and 19874083), the National Key Basic Research Special Foundation, the Natural Science Foundation of Guangdong Province, and the Natural Science Foundation of Education Ministry of China.

[1] A. Ashkin, Phys. Rev. Lett. **40**, 729 (1978).
[2] Michael M. Burns, Jean-Marc Fournier, and Jene A. Golovchenko, Phys. Rev. Lett. **63**, 1233 (1989).
[3] Michael M. Burns, Jean-Marc Fournier, and Jene A. Golovchenko, Science (Washington, DC, U.S.) **249**, 749 (1990).
[4] Cheng Bingying, Hu Wei, Yang Junhui, Li Zhaolin, Zhang Daozhong, and Yang Guozhen, Acta Phys. Sin. (Overseas Ed.) **3**, 681 (1994).
[5] P. Verkerk, B. Lounis, C. Salomon, C. Cohen-Tannoudji, J.Y. Courtois, and G. Grynberg, Phys. Rev. Lett. **68**, 3861 (1992).
[6] B. Lounis *et al.*, Europhys. Lett. **21**, 13 (1993).
[7] M. Campbell, D.N. Sharp, M.T. Harrison, R.G. Denning, and A.J. Turerfield, Nature (London) **404**, 53 (2000).
[8] V. Berger, O. Gauthier-Lafaye, and E. Costard, J. Appl. Phys. **82**, 60 (1997).
[9] E. Yablonovitch, T.J. Gmitter, and K.M. Leung, Phys. Rev. Lett. **67**, 2295 (1997).
[10] N. Katsarakis, E. Chatzitheodoridis, G. Kiriakidis, M.M. Sigalas, C.M. Soukoulis, W.L. Leung, and G. Tuttle, Appl. Phys. Lett. **74**, 3263 (1999).
[11] Dongbin Mei, Bingying Cheng, Wei hu, Zhaolin Li, and Daozhong Zhang, Opt. Lett. **20**, 429 (1998).
[12] K.M. Ho, C.T. Chan, and C.M. Soukoulis, Phys. Rev. Lett. **65**, 3152 (1990).
[13] E. Yablonovitch, J. Opt. Soc. Am. B **10**, 283 (1993).
[14] D.L. Bullok, C.C. Shih, and R.S. Marguiles, J. Opt. Soc. Am. B **10**, 399 (1993).
[15] M.C. Wanke, O. Lehmann, K. Mller, Q.Z. Wen, and M. Stuke, Science (Washington, DC, U.S.) **275**, 1284 (1997).
[16] B.H. Cumpston, Nature (London) **398**, 51 (1999).
[17] C.C. Cheng, *et al.*, J. Vac. Sci. Technol. B **15**, 2764 (1997).
[18] S. Noda, N. Yamamoto, and A. Sasaki, Jpn. J. Appl. Phys., Part 2 **35**, L909 (1996).
[19] J.G. Fleming and S.Y. Lin, Opt. Lett. **24**, 49 (1999).
[20] N.N. Rosanov, Opt. Spectrosc. **75**, 510 (1993).
[21] Jan Masajada and Boguslawa Dubik, Opt. Commun. **198**, 21 (2001).
[22] Wei Hu, Hongqiang Li, Bingying Cheng, Junhui Yang, Zhaolin Li, Jiren Xu, and Daozhong Zhang, Opt. Lett. **20**, 964 (1995).
[23] L.Z. Cai, X.L. Yang, and Y.R. Wang, Opt. Lett. **26**, 1858 (2001).
[24] X.L. Yang, L.Z. Cai, Opt. Commun. **208**, 293 (2002).
[25] W.H. Press, S.A. Teukolsky, W.T. Vetterling, and B.P. Flannery, *Numerical Recipes in C: The Art of Scientific Computing* (Cambridge University Press, Cambridge, 1992), pp. 412–420.